Supporting Information

2D/3D MoS$_2$/TiO$_2$ heterojunction for high-efficiency photothermal catalytic CO$_2$ reduction by phonon heat transfer

Peng Jiang*[a], Xiangyang Jiang* [b] and Yang Yu*[c]

a   State Key Laboratory of Advanced Technology for Materials Synthesis and Processing, Wuhan University of Technology, Wuhan 430070, China

b   Hubei Key Laboratory of Pollutant Analysis and Reuse Technology, College of Chemistry and Chemical Engineering, Hubei Normal University, Huangshi,435002, China

c   Centre for Infrastructure Engineering and Safety, School of Civil and Environmental Engineering, The University of New South Wales, Sydney, NSW 2052, Australia

*Correspondence: PengJiang_edu@163.com (Peng Jiang); jxy@hbnu.edu.cn (Xiangyang Jiang); yang.yu@uts.edu.cn (Yang Yu)

1. Experimental

1.1 Materials

Bulk MoS_2 was purchased from XFNANO Co., Ltd. Titanium butoxide ($C_{16}H_{36}O_4Ti$) was supplied from Shanghai Aladdin Biochemical Technology Co., Ltd. Absolute alcohol was obtained from Sinopharm Chemical Reagent Co., Ltd. All chemicals were used without further purification.

1.2 Synthesis of TiO_2/MoS_2

Firstly, 0.2 g of bulk MoS_2 was dispersed into 100 ml of absolute alcohol by ultrasonic method for 10 min. Then, 4 ml of titanium butoxide was added into the above obtained mixture under magnetic stirring for 12 h. Finally, the mixture was calcinated at 500 °C for 4 h with a ramp rate of 2.0 °C min^{-1} in a muffle furnace to obtain TiO_2/MoS_2. The TiO_2 was prepared in the same way without the addition of MoS_2 powder.

1.3 Characterization

The microstructures of TiO_2, MoS_2, and TiO_2/MoS_2 were examined by FSEM (Hi-tach S-4800) and TEM (Talos F200S). The XRD patterns of TiO_2, MoS_2, and TiO_2/MoS_2 were tested by an X-ray diffraction machine (Bruker D8 Advance) using Cu Kα (λ = 0.15418 nm) radiation. The X-ray photoelectron spectroscopy (XPS, Omicron Sphera II, Germany) data of TiO_2, MoS_2, and TiO_2/MoS_2 were obtained on a mono-chromated Al Kα Xray source (hv=1486.6 eV) at 15 kV/150 W to detect the chemical states of elements in the samples. Nitrogen adsorption isotherms and Brunauer-Emmett-Teller (BET) surface area of TiO_2, MoS_2, and TiO_2/MoS_2 were performed on a nitrogen adsorption apparatus (TriStar II 2020). The UV–vis diffuse reflectance spectra (UV–vis DRS) of TiO_2, MoS_2, and TiO_2/MoS_2 were measured by UV–VIS-NIR spectrometer (Lambda 750S, PerkinElmer) over a range of 200–800 nm. Transient photo-current spectra (TPC), electrochemical impedance spectroscopy (EIS), and the Mott-Schottky (M-S) curve of TiO_2, MoS_2, and TiO_2/MoS_2 were acquired on an electro-chemical workstation (CS2350H, CorrTest) in 0.5 M Na2SO4 solution at room temperature using a 300W Xenon lamp (PLS-SXE300, PerfectLight). The Pt plate and Ag/AgCl were employed as the counter electrode and the reference electrode,

respectively. In-situ time-resolved DRIFT spectra of TiO_2/MoS_2 were tested by a Fourier transform infrared spectrometer (VERTEX V80, Bruker). The steady-state and time-resolved photoluminescence (PL) spectra of TiO_2 and TiO_2/MoS_2 were recorded on a Spectrophotometer (F-4700 FL, Hitachi) at a voltage of 700V. The work functions of TiO_2 and MoS_2 were calculated by density functional theory (DFT) in Materials Studio.

1.4 Photocatalytic CO_2 reduction

50 mg of catalyst was placed into a stainless steel reactor with an optical quartz window at the top. The reactor was firstly vacuumed, and then CO_2 and H_2 were introduced into the stainless steel reactor at a volume ratio of 1:4 for half an hour to blow out the air in the reactor. A 300 W Xenon lamp (PLS-SXE300, Beijing Perfect-Light) with a filter (AM 1.5 G, Ceaulight Technology Co. Ltd., China) was employed to simulate solar illumination with about 100 $mW·cm^{-2}$. The reactor was irradiated by a Xenon lamp for the desired time. During the photocatalytic reaction process, the gaseous mixture is periodically sampled from the stainless steel reactor every 0.5 hour and analyzed by gas chromatography.

2. DFT calculation

DFT calculation was performed by using the CASTEP module. The exchange-correlation interaction was described by generalized gradient approximation (GGA) with the Perdew–Burke–Ernzerhof (PBE) functional. The energy cutoff was set to 570 eV. The Monkhorst-Pack k-point mesh was set as $3 \times 3 \times 1$. A vacuum space with a thickness of 20 Å was used to eliminate interactions between periodic structures.
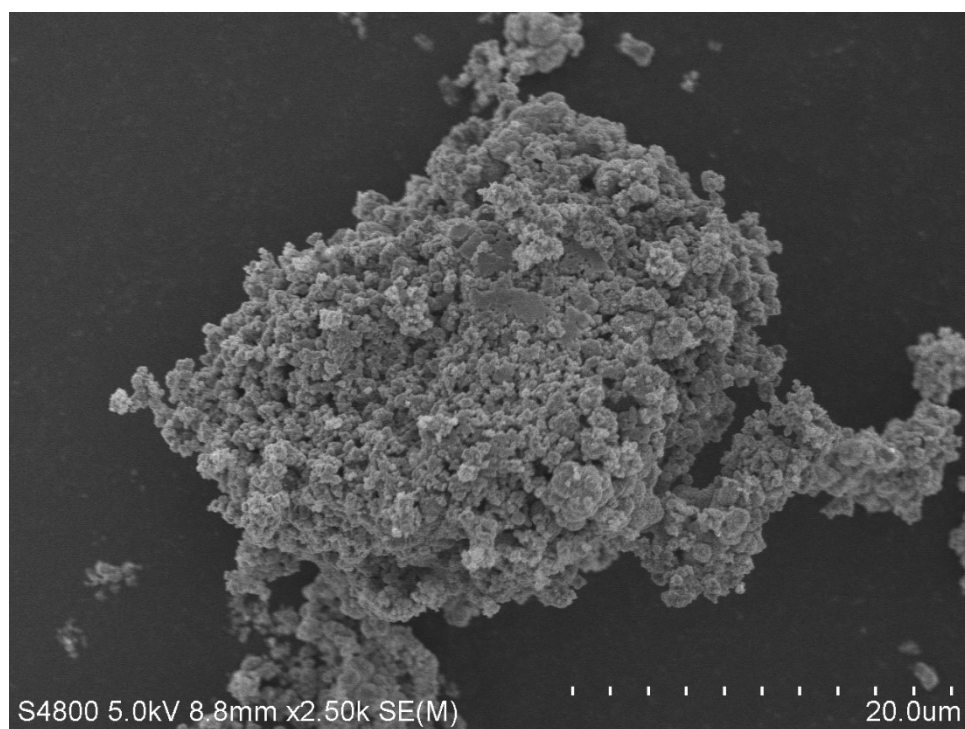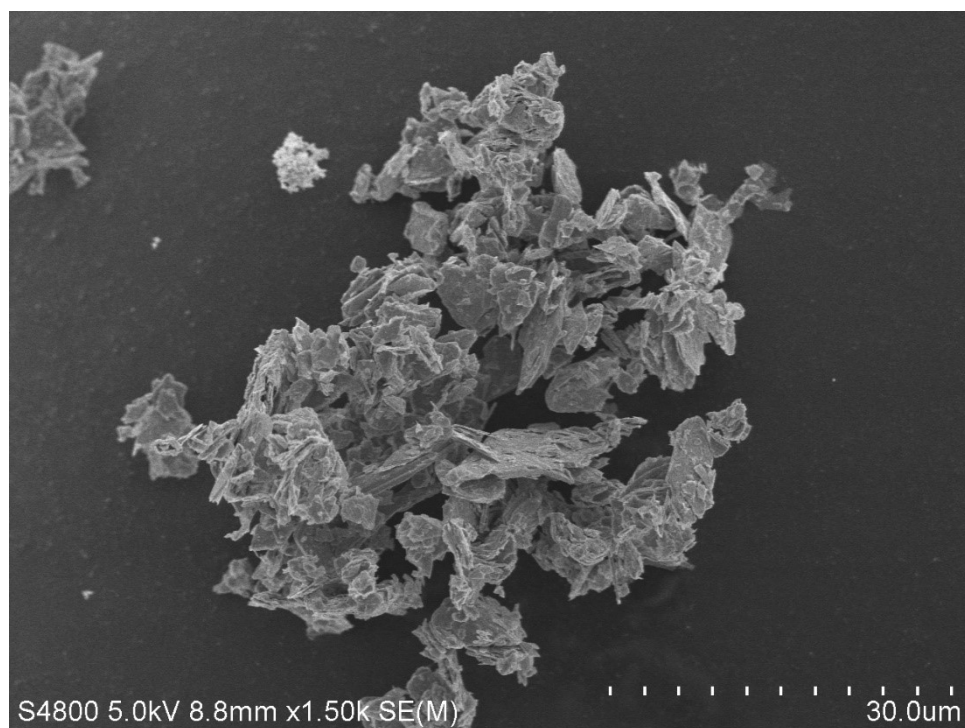
Fig. S1. FSEM image of TiO$_2$.
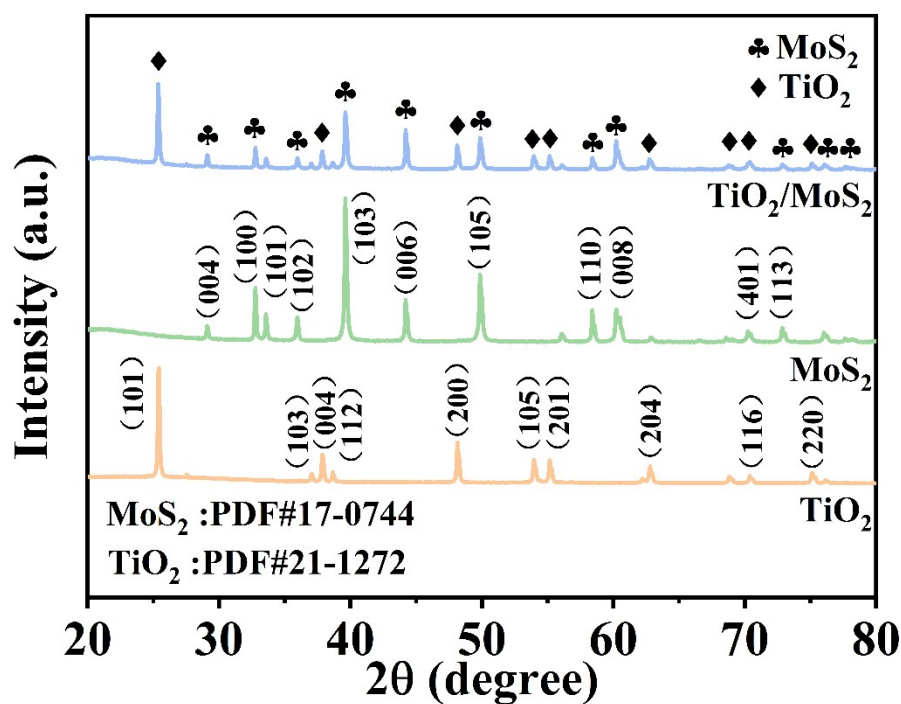

Fig. S2. FSEM image of MoS$_2$.

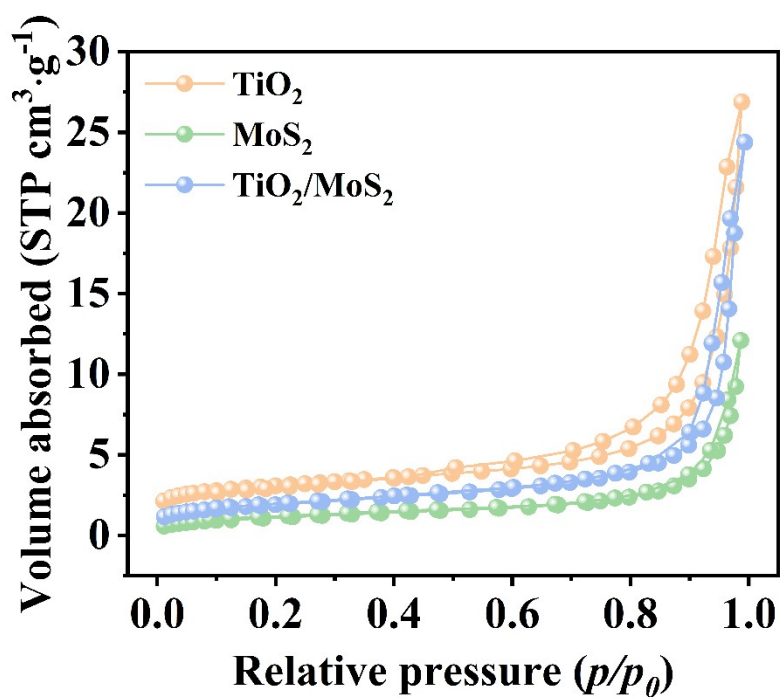Fig. S3. XRD patterns of TiO_2, MoS_2, and TiO_2/MoS_2.

Fig. S4. Nitrogen adsorption-desorption isotherm of TiO_2, MoS_2, and TiO_2/MoS_2.
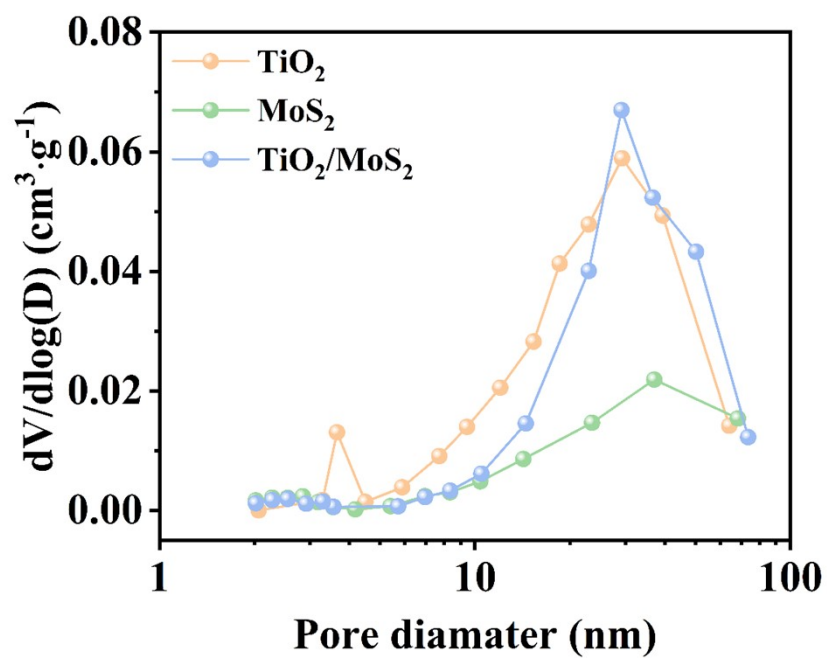
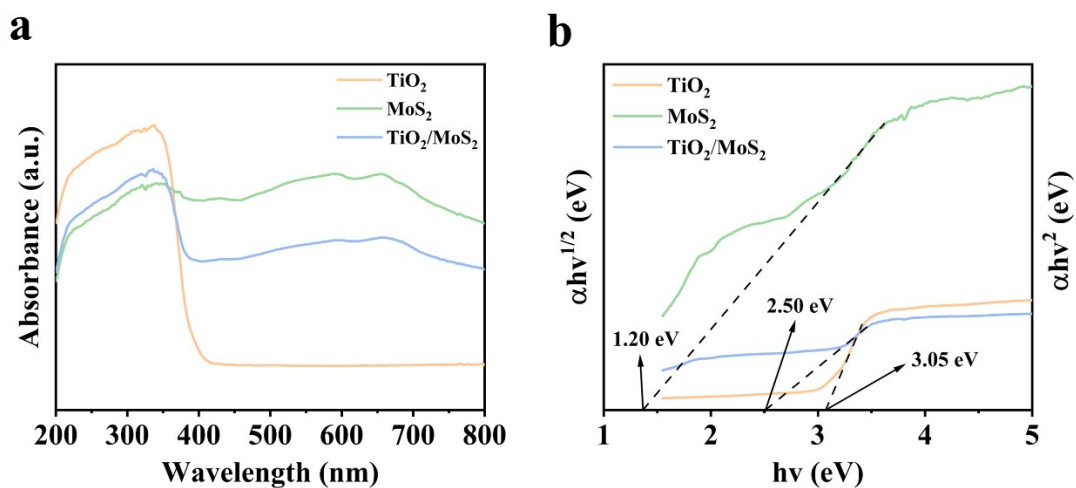Fig. S5. Pore-size distribution curves of TiO_2, MoS_2, and TiO_2/MoS_2.

Fig. S6. (a) UV-vis DRS and (b) Tauc plots of TiO$_2$, MoS$_2$, and TiO$_2$/MoS$_2$.
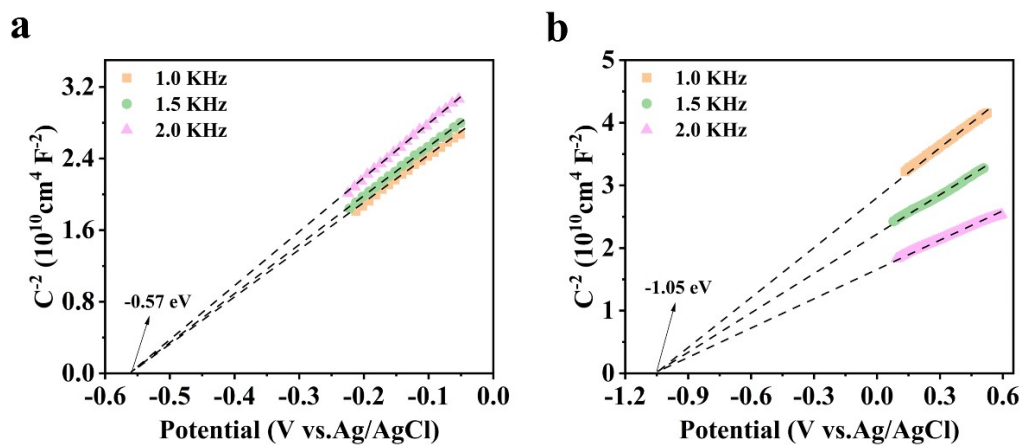

Fig. S7. M-S plots of (a) TiO$_2$ and (b) MoS$_2$.

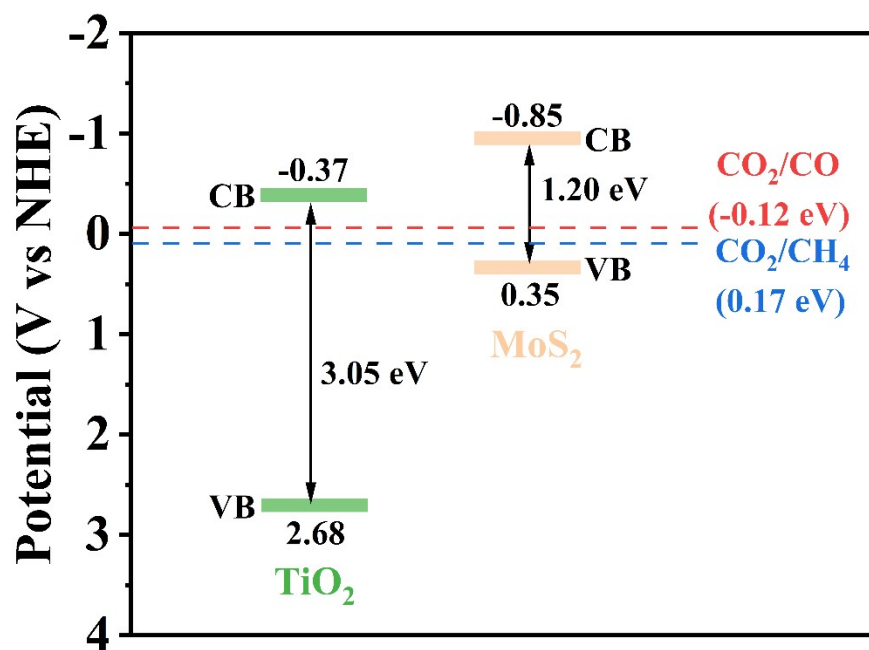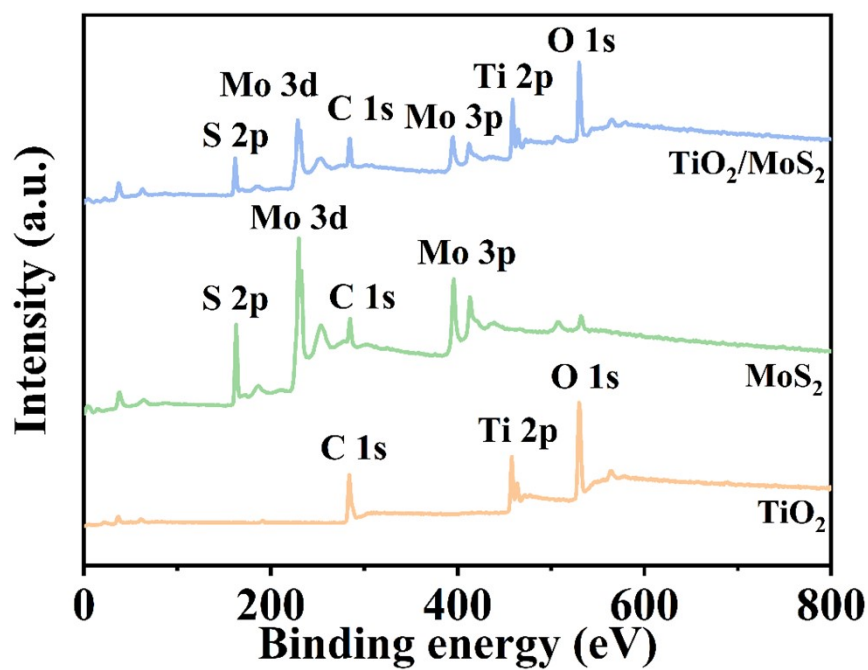Fig. S8. Estimated band structures of TiO_2 and MoS_2.

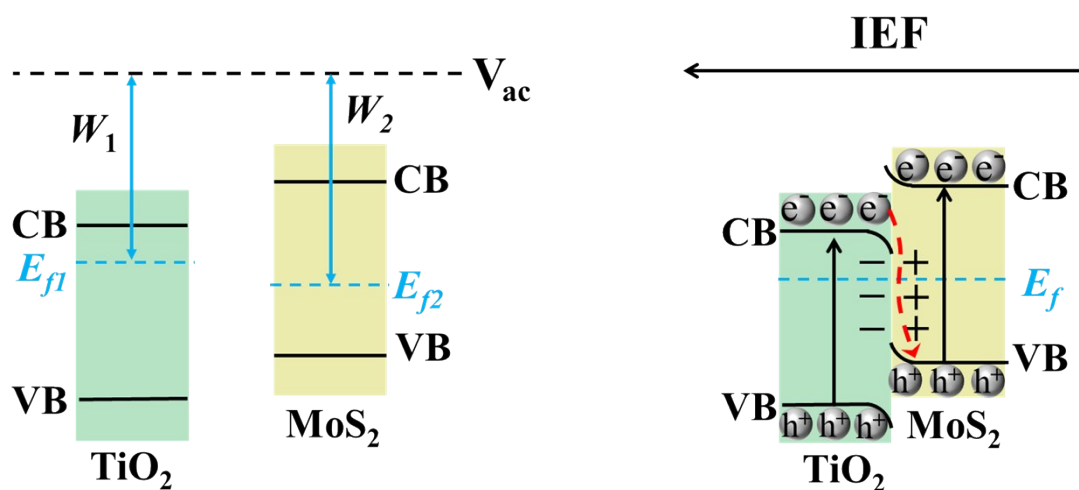Fig. S9. XPS survey spectra of TiO_2, MoS_2, and TiO_2/MoS_2.

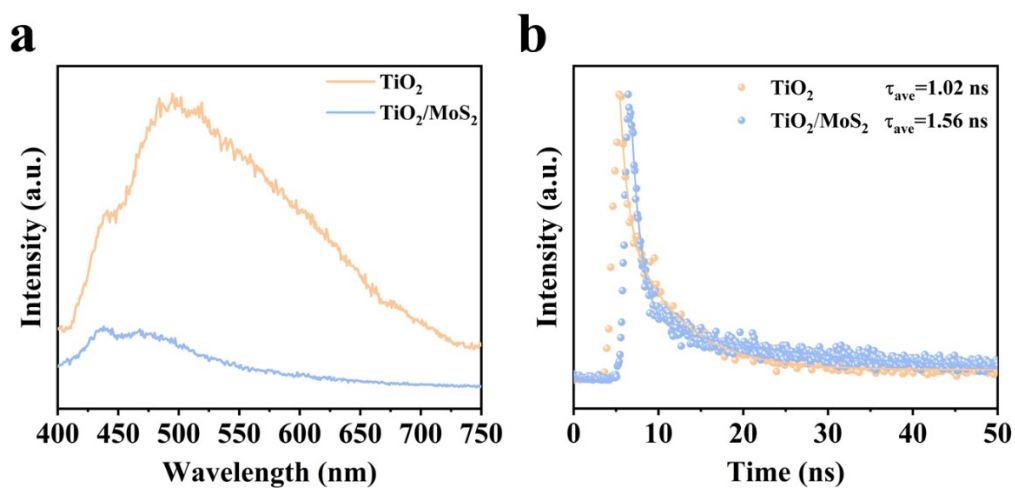Fig. S10. Schematic illustrations of the electron transfer mechanism between TiO_2 and MoS_2.

Fig. S11. (a) steady-state photoluminescence (PL) spectra, (b) time-resolved PL spectra of TiO_2 and TiO_2/MoS_2.
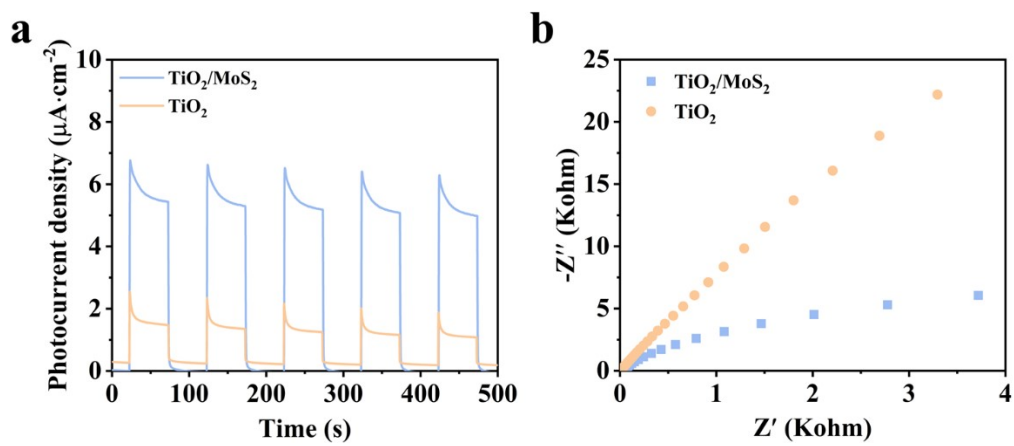
Fig. S12. (a) Transient photocurrent spectra (TPC) and (b) electrochemical impedance spectroscopy (EIS) spectra of TiO_2 and TiO_2/MoS_2.

Table S1. Brunauer–Emmett–Teller surface areas (S_{BET}) of samples.

Catalyst	S_{BET} $(m^2 \cdot g^{-1})$
TiO_2	11.2
MoS_2	4.0
TiO_2/MoS_2	6.9

Table S2. Performance comparison of TiO_2-based and MoS_2-based photocatalytic materials for CO_2 reduction.

Photocatalysis	Light source	Product	Yield ($\mu mol \cdot g^{-1} \cdot h^{-1}$)	Reference
MoS_2/TiO_2	300 W Xe lamp	CH_4	30.42	**This work**
		CO	8.25	
MoS_2/TiO_2 physical mixture	300 W Xe lamp	CH_4	10.01	**This work**
		CO	3.31	
$SiO_2@TiO_2$	300 W Xe lamp	CH_4	13.21	1
$TiO_2/Ti_3C_2/Cu$	300 W Xe lamp	CO	1.17	2
		CH_4	12.5	
$Cu_{0.7}Au_{0.3}/TiO_2$	300 W Xe lamp	CO	6.08	3
$(PdCu)_2–TiO_2$	300 W Xe lamp	CH_4	18.1	4
$rGO–MoS_2/PPy$	300 W Xe lamp	CH4	1.50	5
		CO	3.95	
$MoS_2@NH_2$-MIL-68	300 W Xe lamp	CH_4	3.14	6

References

1 J. S. Li, C. Cao, X. Y. Zhang, H. H. Dong, M. F. Wang, L. Zhang and Z. H. Xing, Carbon Energy., https://doi.org/10.1002/cey2.700.

2 W. Y. Xu, Y. H. Peng, D. Hu, I. Razanau, D. Gu and W. Xiao. ChemCatChem., 2024, 20, e202400873.

3 X. W. Mu, Q. H. Xu, Y. Xie, Y. C. Ma, Z. Q. Zhang, Z. Shen, Y. Guo, J. Yu, S. Ajmal, W. Zhang and J. Zhao, J. Alloy. Compd., 2024, 980, 173589.

4. Y. Liu, S. J. Sun, M. Ma, X. Y. Zhong, F. Y. Gao, G. T. Hai and X. B. Huang, J. Mater. Chem. A., 2024, 12, 23577-23589.

5 N. Kumar, S. Kumar, R. Gusain, N. Manyala, S. Eslava and S. Ray, ACS Appl. Energy. Mater., 2020, 10, 9897–9909.

6 X. Wang, J. He, L. Mao, X. Y. Cai, C. Z. Sun and M. S. Zhu. CHEM. ENG. J., 2021, 416, 128077.